Available online at www.sciencedirect.com
ScienceDirect
Materials Research Bulletin 42 (2007) 1531–1538
Materials Research Bulletin
www.elsevier.com/locate/matresbu

Synthesis, structure and magnetic properties of a new iron phosphonate-oxalate with 3D framework: $[Fe(O_3PCH_3)(C_2O_4)_{0.5}(H_2O)]$

Yang-Yang Zhang, Yue Qi, Ying Zhang, Zi-Yu Liu, Yin-Feng Zhao, Zhong-Min Liu *

Applied Catalysis Laboratory, Dalian Institute of Chemical Physics, Chinese Academy of Sciences, Dalian 116023, PR China

Received 14 July 2006; received in revised form 23 October 2006; accepted 26 October 2006
Available online 1 December 2006

Abstract

A new iron phosphonate-oxalate $[Fe(O_3PCH_3)(C_2O_4)_{0.5}(H_2O)]$ (**1**), has been synthesized under hydrothermal condition. The single-crystal X-ray diffraction studies reveal that **1** consists of layers of vertex-linked FeO_6 octahedra and O_3PC tetrahedra, which are further connected by bis-chelate oxalate bridges, giving to a 3D structure with 10-membered channels. Crystal data: monoclinic, $P2_1/n$ (no. 14), $a = 4.851(2)$ Å, $b = 16.803(7)$ Å, $c = 7.941(4)$ Å, $\beta = 107.516(6)^\circ$, $V = 617.2(5)$ Å^3, $Z = 4$, $R_1 = 0.0337$ and $wR_2 = 0.0874$ for 1251 reflections [$I > 2\sigma(I)$]. Mössbauer spectroscopy measurement confirms the existence of high-spin Fe(III) in **1**. Magnetic studies show that **1** exhibits weak ferromagnetism with $T_N = 30$ K due to a weak spin canting.

Keywords: A. Magnetic materials; C. Mössbauer spectroscopy; D. Crystal structure; D. Magnetic properties

1. Introduction

Recently, many research activities have focused on the design and synthesis of open-framework transition metal phosphonates, not only due to their intriguing structural motifs but also their potential applications in catalysis, host–guest chemistry and the promising photo-, electro- and magnetic properties [1–3]. During the past decades, many open-framework metal phosphonates have been synthesized through use of multifunctional phosphonates owing to their versatile connection modes with transitional metal centers [4,5]. More recently, the strategy, i.e. introduction of a second organic ligand into the structure of metal phosphonate, has been proved to be an effective method for constructing open-framework metal phosphonate. This strategy can present the following advantages: (1) the introduced second organic ligand usually serves as chelating and bridging unit that can facilitate the formation of extended structure; (2) from a magnetic point of view, such mixed-ligand metal phosphonates are particularly interesting as they offer possibilities for rationally designing new magnetic materials by selection of appropriate second ligand. However, it was well known that the syntheses of compounds containing mixed ligands are expected to

* Corresponding author. Tel.: +86 411 84685510; fax: +86 411 84685510.
E-mail address: liuzm@dicp.ac.cn (Z.-M. Liu).

0025-5408/$ – see front matter © 2006 Elsevier Ltd. All rights reserved.
doi:10.1016/j.materresbull.2006.10.027

be more difficult than those of compounds containing one ligand; therefore, only a few mixed-ligand metal phosphonates have been synthesized, such as Sn [6,7], Cu [8–11], Co [12–14], Zn [14], Pb [15] and Ga [16] compounds. We have been interested to investigate the formation of mixed-ligand metal phosphonates employing hydrothermal methods. During the course of these investigations, we have now isolated a new iron phosphonate-oxalate $[Fe^{III}(O_3PCH_3)(C_2O_4)_{0.5}(H_2O)]$ (**1**), possessing a 3D open framework with 10-membered channels and exhibiting weak ferromagnetism at $T_N = 30$ K. As far as we are aware, the compound **1** is the first example of iron phosphonate-oxalate system.

2. Experimental

2.1. Synthesis and characterization

The iron phosphonate-oxalate, **1**, was hydrothermally synthesized in a Teflon-lined stainless steel autoclave with 23 mL capacity under autogenous pressure. Oxalate (0.64 g, 5 mmol) and methylphosphonic acid (0.96 g, 10 mmol) were dispersed into the aqueous solution (10 mL) of iron chloride (1.35 g, 5 mmol). Under continuous stirring, 0.69 g of ethylenediamine was added dropwise to the above solution until a pH of 2.3 was achieved. The final mixture was transferred into the autoclave and heated at 110 °C for 144 h. After the autoclave was cooled slowly down to room temperature at the rate of 25 °C h^{-1}, transparent light-brown crystals of **1** were recovered by filtration, washed with deionized water, and dried at room temperature (68% yield based on Fe). The powder XRD pattern of the crystals indicated that as-synthesized product was a new material; the pattern was entirely consistent with the simulated one from single-crystal X-ray diffraction (Fig. 1). Anal. Calc. for $C_2H_5PO_6Fe$ (%): Fe 26.35, P 14.62, C 11.34, H 2.38;

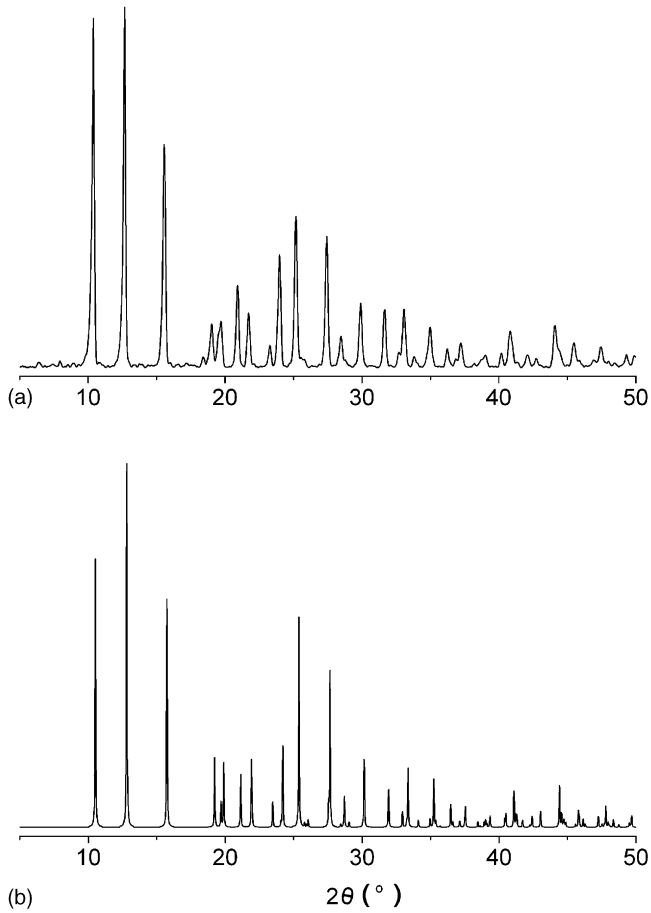

Fig. 1. Experimental powder XRD pattern (a) of **1** and simulated one (b).

found Fe 26.20, P 15.00, C 11.37, H 2.54; IR (KBr), $\tilde{\nu}$ = 3213 (s), 3004 (w), 2943 (w), 1690 (s), 1416 (w), 1359 (m), 1310 (m), 1139 (s), 1071 (s), 997 (s), 787 (m), 742 (m), 548 (m) and 473 (m).

Powder XRD data were collected on a D/MAX-b X-ray diffractometer with Cu Kα radiation operating at 40 kV and 100 mA. Elemental analyses (C and H) were performed on an Elementar Vario EL analyser and the Fe and P contents were analyzed by inductively coupled plasma atomic emission spectrometer (ICP-AES) (TJA, Iris Advantage). FT-IR spectra were recorded on a Bruker EQUINOX 55 FT-IR spectrometer using KBr pellets in the range 4000–400 cm^{-1}. Mössbauer spectra were obtained with a constant acceleration spectrometer using a room-temperature ^{57}Co/Pd source in the transmission geometry. Isomer shift values are calculated based on an iron foil standard. The magnetic measurements were carried out with Quantum Design SQUID MPMS XL-7 instruments. The diamagnetism of the sample and sample holder were taken into account.

2.2. Single-crystal X-ray diffraction

A suitable single crystal of dimensions 0.08 mm × 0.06 mm × 0.04 mm was mounted on a Bruker SMART CCD diffractometer equipped with a graphite-monochromated Mo Kα radiation (λ = 0.71073 Å) at 293 K using the ω–2θ scan technique. The intensity data collection was performed by a CCD area detector at room temperature in the θ range of 2.42–26.38°. Semiempirical absorption corrections were carried out using the SADABS program. Other effects, such as absorption by the glass fibres, were simultaneously corrected. The structure was solved by direct methods and refined by full-matrix least-squares fitting on F^2 by SHELXL-97 [17]. All non-hydrogen atoms were located from the initial solution and refined with anisotropic thermal parameters. The hydrogen atoms were positioned geometrically and refined with fixed isotropic thermal parameters. Bond-valence calculation results indicate all iron atoms are trivalent [18]. The crystallographic data, the main bond lengths and angles are listed in Tables 1 and 2, respectively. The CIF file has been deposited in the Cambridge Crystallographic Data Centre (Deposit CCDC 233213).

3. Results and discussion

3.1. Crystal structure description

The iron phosphonate-oxalate, **1**, has a 3D open-framework constructed by FeO_6 octahedra, O_3PC tetrahedra and bis-chelate oxalate building blocks. The asymmetric unit of **1** contains 10 non-hydrogen atoms, of which there are 1 crystallographically independent iron and 1 phosphorus atom. Each iron atom is in a slightly distorted octahedral FeO_6 coordination, with Fe–O bond lengths in the range from 1.878(2) to 2.108(2) Å. Three coordination sites of it are occupied by phosphonate oxygens from three different methylphosphonic acid; the fourth and fifth oxygens are

Table 1
Crystallographic data for $[Fe(O_3PCH_3)(C_2O_4)_{0.5}(H_2O)]$

Empirical formula	$C_2H_5FeO_6P$
Formula weight	211.88
T (K)	293(2)
Crystal system	Monoclinic
Space group	$P2_1/n$
a (Å)	4.851 (2)
b (Å)	16.803(7)
c (Å)	7.941(4)
β (°)	107.516(6)
V (Å^3)	617.2 (5)
Z	4
$D_{calcd.}$ (g cm^{-3})	2.280
F (0 0 0)	424
Minimum and maximum transmission	0.725672/1.000,000
Goodness-of-fit	1.134
R [$I > 2\sigma(I)$]	$R_1 = 0.0337$, $wR_2 = 0.0874$
R [all data]	$R_1 = 0.0404$, $wR_2 = 0.0903$

$R_1 = \sum||F_o|-|F_c||/\sum|F_o|$; $wR_2 = [\sum w(F_o^2 - F_c^2)^2 / \sum w(F_o^2)^2]^{1/2}$.

Table 2
Selected bond lengths (Å) and angles (°) in $[Fe(O_3PCH_3)(C_2O_4)_{0.5}(H_2O)]$

Fe(1)–O(1)	1.918(2)	Fe(1)–O(2)[a]	1.878(2)
Fe(1)–O(3)[b]	1.936(2)	Fe(1)–O(4)	2.108(2)
Fe(1)–O(5)[c]	2.100(2)	Fe(1)–O(6)	2.060(2)
P(1)–O(1)	1.503(2)	P(1)–O(2)	1.515(2)
P(1)–O(3)	1.534(2)	P(1)–C(1)	1.771(4)
C(2)–O(4)	1.245(4)	C(2)–O(5)	1.244(4)
C(2)–C(2)[c]	1.524(6)		
O(2)[a]–Fe(1)–O(1)	97.53(10)	O(2)[a]–Fe(1)–O(3)[b]	101.48(10)
O(1)–Fe(1)–O(3)[b]	93.27(10)	O(2)[a]–Fe(1)–O(6)	87.57(10)
O(1)–Fe(1)–O(6)	170.67(10)	O(3)[b]–Fe(1)–O(6)	93.36(10)
O(2)[a]–Fe(1)–O(5)[c]	164.94(9)	O(1)–Fe(1)–O(5)[c]	91.20(10)
O(3)[b]–Fe(1)–O(5)[c]	90.18(9)	O(6)–Fe(1)–O(5)[c]	82.22(9)
O(2)[a]–Fe(1)–O(4)	91.04(10)	O(1)–Fe(1)–O(4)	86.04(10)
O(3)[b]–Fe(1)–O(4)	167.44(9)	O(6)–Fe(1)–O(4)	86.06(10)
O(5)[c]–Fe(1)–O(4)	77.30(8)	O(1)–P(1)–O(2)	111.80(14)
O(1)–P(1)–O(3)	111.62(13)	O(2)–P(1)–O(3)	108.96(13)
O(1)–P(1)–C(1)	108.01(17)	O(2)–P(1)–C(1)	107.26(17)
O(3)–P(1)–C(1)	109.06(16)	O(5)–C(2)–O(4)	127.3(3)
O(5)–C(2)–C(2)[c]	116.8(3)	O(4)–C(2)–C(2)[c]	115.9(3)

Symmetry transformations used to generate equivalent atoms.
[a] $x + 1/2, -y + 1/2, z + 1/2$.
[b] $x + 1, y, z$.
[c] $-x + 2, -y, -z + 2$.

donated by a bis-chelate oxalate ligand; while the apical position is occupied by one water molecule oxygen atom. Each phosphorus atom adopts tetrahedral O_3PC geometry, showing the expected average bond lengths and angles. Such O_3PC tetrahedron shares three of its corners with three neighbouring FeO_6 octahedra, thus forming a 2D corrugated layer possessing uniform 6-membered rings in the *ac*-plane (Fig. 2a). It is worthy to note that layers exclusively possessing 6-membered apertures are rare [19,20]. As shown in Fig. 2b, these 2D layers are cross-linked by oxalate units to give rise to a 3D structure with unidimensional channels running along the *a*-axis. The channel has a 10-membered window formed by six FeO_6, four O_3PC, and two oxalate units. In this window, the longest Fe···Fe distance is 12.950 Å whereas the shortest one is 5.507 Å. But the free diameter is reduced due to the channel apertures

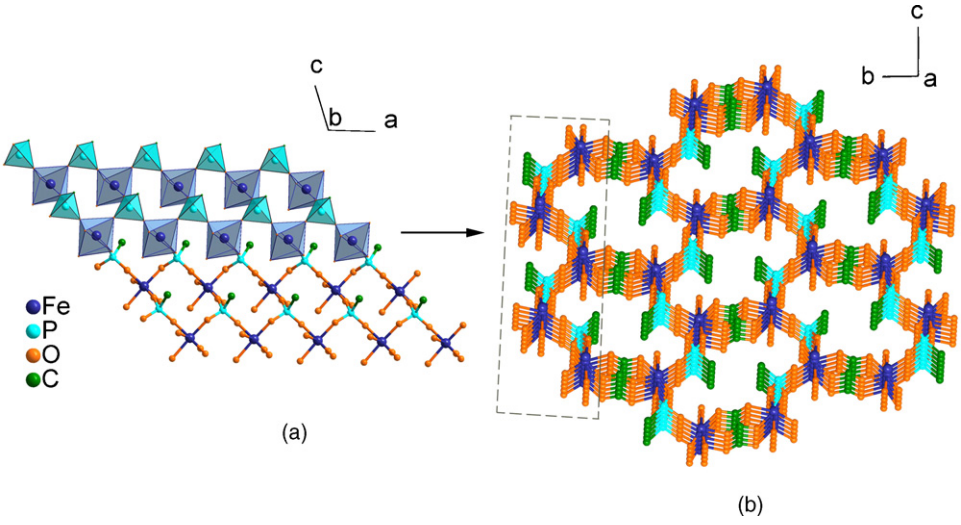

Fig. 2. (a) The 6-membered ring layer in the *ac*-plane constructed from alternating FeO_6 and O_3PC units. (b) 3D structure of **1** along *a*-axis, showing the 10-membered channels. The hydrogen atoms are omitted for clarity.

accommodating both methyl groups and coordination water molecules attached to iron ions. In addition, the coordination water molecules induce strong hydrogen bonding with the oxygen atoms of oxalate and methylphosphonic acid. The short donor–acceptor (O···O) distances and nearly linear O–H···O angles are measured to be ca. 2.668–2.781 Å and 165.1–167.9°.

It is interesting to observe that the ethylenediamine could not be incorporated in the crystal structure of **1**, though it was added in the starting mixture. To explore the effects of ethylenediamine, we attempted to use other alkyl amines instead of ethylenediamine, and also obtained crystals of **1** in smaller crystal size. However, it must be emphasized that no material like **1** has been formed in the absence of such usage of alkyl amines in the starting mixture.

3.2. Mössbauer spectroscopy

The room temperature ^{57}Fe-Mössbauer spectroscopy for **1** shows a paramagnetic doublet (Fig. 3). The determined isomer shift (IS) value is ca. 0.429 mm s^{-1}, which is characteristic of high-spin Fe(III). According to Menil [21], the usual range of isomer shifts in oxides is 0.29–0.50 mm s^{-1} for Fe(III) with six-coordination. In addition, a little distortion exists in these FeO_6 octahedral configurations deduced from the absolute values of quadrupole splitting (QS) of 0.376 mm s^{-1}. Therefore, the valence of the iron atoms in **1** is also confirmed by Mössbauer spectroscopy.

3.3. Magnetic properties

The temperature-dependent magnetic susceptibility of **1** was measured at a field of 1000 Oe in 2–300 K. Above 70 K, the magnetic behavior of **1** follows the Curie–Weiss law ($C = 4.65$ cm^3 K mol^{-1}, $\theta = -77.4$ K), indicating a significant antiferromagnetic coupling between the Fe(III) ions. The room-temperature χ_m value is 1.22×10^{-2} cm^3 mol^{-1}, corresponding to an effective magnetic moment of 5.42 μ_B per Fe(III) ion, which is slightly smaller than the theoretical high-spin Fe(III) (5.92 μ_B). Upon cooling, χ_m versus T plot shows an incipient maximum centered at 40 K, and an abrupt increase below 30 K (Fig. 4). The final increase in χ_m value at lower temperatures is characteristic of a weak ferromagnet, in which a predominantly antiferromagnetic phase possesses a small spontaneous ferromagnetic ordering due to the spin canting [22–27]. Further support for this comes from that χ_m versus T curves at different fields show pronounced field dependence of the low-temperature phase (inset in Fig. 4) [23–27]. As the field is lowered, the apparent ferromagnetic increase in χ_m can is observed below ca. 30 K. However, as a field greater than 5000 Oe, this increase virtually disappears, which indicates that this spontaneous moment is destroyed, rendering a typical antiferromagnet.

Weak ferromagnetic magnetic order is also clearly evident from ac susceptibility measurements (Fig. 5). The maximum of χ'_m observed at $T_N = 30$ K, in agreement with the above results, confirms the occurrence of an

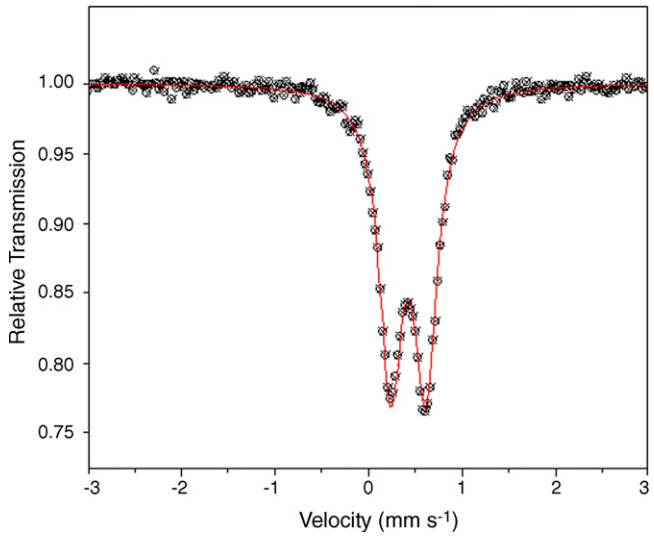

Fig. 3. Mössbauer spectra of **1** at room temperature.

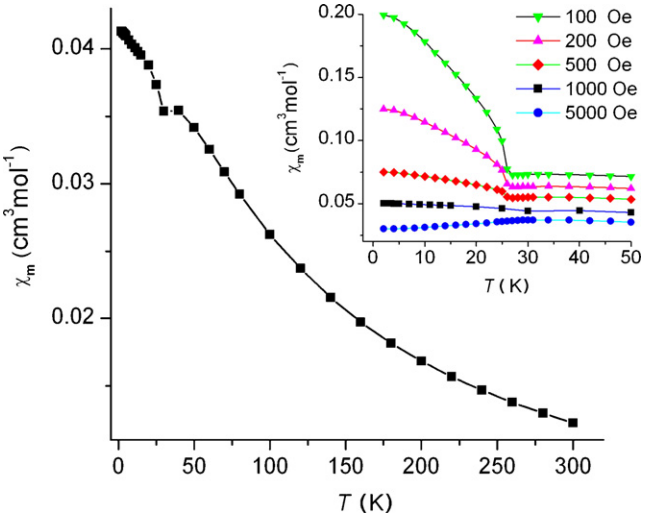

Fig. 4. The temperature dependence of χ_m for **1** measured at 1000 Oe; Inset: χ_m vs. T plots at different fields.

antiferromagnetic phase transition. No detected out-of-phase signal and frequency dependence was observed. Furthermore, hysteresis loop for **1** measured at 2 K is characteristic of a soft magnet with a small coercive field of 445 Oe and a remnant magnetization of 0.002 Nβ mol^{-1} (Fig. 6).

As insight into the structure of **1** based on the magnetic point, the magnetic Fe(III) ions are situated at the corners of a 3D network (Fig. 7a). It has been shown that the intralayer interactions between Fe(III) ions can be mediated by three kinds of O–P–O bridges, forming a triangle-like planar array (Fig. 7b). Correspondingly, the Fe···Fe distances via O–P–O exchange bridges are ca. 4.851, 5.020 and 6.066 Å, respectively. On the other hand, the interlayer coupling is mediated by the oxalate bridges with the Fe···Fe distance of 5.507 Å. According to some previous studies based on Fe(III)-phosphonate and Fe(III)-oxalate system, both intra- and interlayer exchange bridges of **1** are expected to transmit antiferromagnetic coupling, whereas the observation of the weak ferromagnetism in **1** is due to spin canting [28–32]. Generally, two mechanisms for producing the canted spin structure have been suggested: (1) single-ion magnetic anisotropy; (2) the antisymmetric Dzyaloshinsky–Moriya (DM) exchange coupling [33–35]. The second one has to be responsible for the canting in **1**, because of the isotropic character of the high-spin Fe(III) ion. It is reasonable to expect that the spontaneous moment arises from an antisymmetric DM interaction, because the compound **1** lacks a center of symmetry between Fe(III) ions through O–P–O bridges and possesses distorted coordination environments.

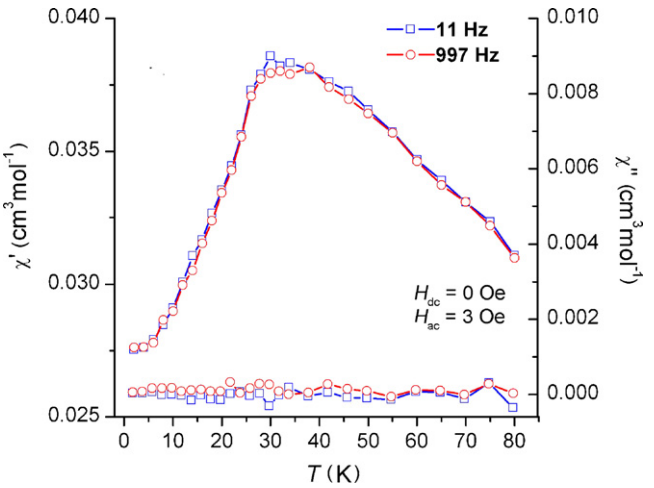

Fig. 5. The temperature dependence of ac magnetic susceptibility (upper: χ'_m, lower: χ''_m) for **1**.

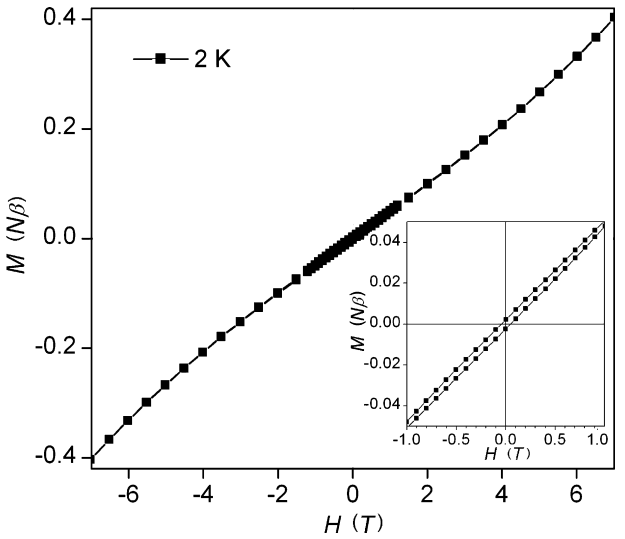

Fig. 6. A narrower hysteresis loop for **1**, recorded at 2 K.

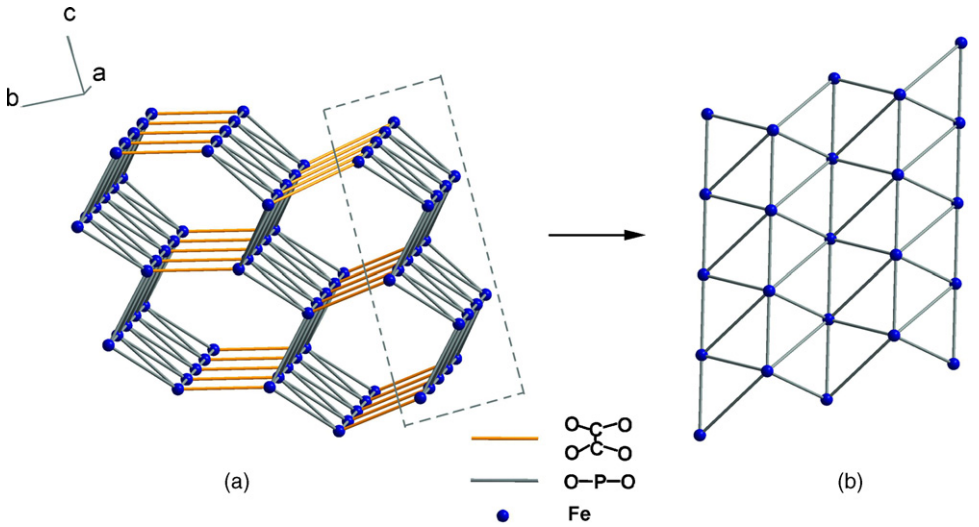

Fig. 7. (a) Schematic diagram showing 3D magnetic network of **1**; (b) view of the triangular-like magnetic layer in the *ac*-plane, showing each metal ion interacts with its six nearest neighbors.

4. Conclusions

The synthesis, the structure and the magnetic properties of a new iron phosphonate-oxalate $[Fe(O_3PCH_3)(C_2O_4)_{0.5}(H_2O)]$ (**1**), possessing methylphosphonic acid and oxalate units in the same framework have been accomplished. This work shows that the introduction of a second ligand provides the potential to produce high-dimension networks and interesting magnetic properties. In addition, it is also interesting work to investigate the role of the amines in the formation of open-framework structure of **1**. It is worthy to note that the compound **1** was found to be similar structure topology to the corresponding iron phosphate-oxalate $[Fe^{III}_2(H_2O)_2(HPO_4)_2(C_2O_4)]\cdot H_2O$ [19]. The reported compound was constructed by FeO_6 octahedra, inorganic PO_4 tetrahedra and oxalate building units. Although two compounds have the similar structure topology, the compound **1** exhibits weak ferromagnetism at $T_N = 30$ K, while the reported compound shows antiferromagnetic ordering. Their magnetization measurements were carried out in the 30–300 K temperature range. We believed that low-field and low-temperature magnetization

measurements will contribute to characterize to overall magnetic behavior of the reported compound. Now we are currently pursuing this work for a better understanding of the difference and its origin.

Acknowledgments

This work was supported by the fund from the Knowledge Innovation Program of the Chinese Academy of Sciences (DICP K2000B3). The authors thank Dr. H.-B. Song at NanKai University for crystal structure determination, Prof. H.-B. Huang at NanJing University for Mössbauer analysis and Dr. W.-X. Zhang at Sun Yat-Sen University for magnetic measurement.

References

[1] A. Clearfield, in: K.D. Karlin (Ed.), Progress in Inorganic Chemistry, vol. 47, Wiley, New York, 1998, p. 371.
[2] K. Maeda, Micropor. Mesopor. Mater. 73 (2004) 47.
[3] C. Bellitto, in: J.S. Miller, M. Drillon (Eds.), Magnetism: Molecules to Materials II, VCH, New York, 2001, p. 425.
[4] D.L. Lohse, S.C. Sevov, Angew. Chem. Int. Ed. Engl. 36 (1997) 1619.
[5] J.-G. Mao, Z. Wang, A. Clearfield, Inorg. Chem. 41 (2002) 2334.
[6] B. Adair, S. Natarajan, A.K. Cheetham, J. Mater. Chem. 8 (1998) 1477.
[7] N. Stock, G.D. Stucky, A.K. Cheetham, Chem. Commun. (2000) 2277.
[8] P. Yin, L.-M. Zheng, S. Gao, X.-Q. Xin, Chem. Commun. (2001) 2346.
[9] L.-M. Zheng, P. Yin, X.-Q. Xin, Inorg. Chem. 41 (2002) 4084.
[10] P. Yin, Y. Peng, L.-M. Zheng, S. Gao, X.-Q. Xin, Eur. J. Inorg. Chem. (2003) 726.
[11] R.-B. Fu, X.-T. Wu, S.-M. Hu, W.-X. Du, J.-J. Zhang, Z.-Y. Fu, Inorg. Chem. Commun. 6 (2003) 694.
[12] R.-B. Fu, X.-T. Wu, S.-M. Hu, J.-J. Zhang, Z.-Y. Fu, W.-X. Du, Inorg. Chem. Commun. 6 (2003) 827.
[13] J.-L. Song, A.V. Prosvirin, H.-H. Zhao, J.-G. Mao, Eur. J. Inorg. Chem. 18 (2004) 3706.
[14] J.-L. Song, H.-H. Zhao, J.-G. Mao, K.R. Dunbar, Chem. Mater. 16 (2004) 1884.
[15] J.-L. Song, J.-G. Mao, Y.-Q. Sun, A. Clearfield, Eur. J. Inorg. Chem. (2003) 4218.
[16] C.H. Lin, K.H. Lii, Inorg. Chem. 43 (2004) 6403.
[17] G.M. Sheldrick, SHELXL-97, Program for the Refinement of Crystal Structures, University of Göttingen, Göttingen, Germany, 1997.
[18] I.D. Brown, D. Altermatt, Acta Cryst. B41 (1985) 244.
[19] A. Choudhury, S. Natarajan, C.N.R. Rao, Chem. Eur. J. 6 (2000) 1168.
[20] S. Natarajan, J. Solid State Chem. 139 (1998) 200.
[21] F. Menil, J. Phys. Chem. Solids 46 (1985) 763.
[22] C. Bellitto, F. Federici, M. Colapietro, G. Portalone, D. Caschera, Inorg. Chem. 41 (2002) 709, and references therein.
[23] S.O.H. Gutschke, D.J. Price, A.K. Powell, P.T. Wood, Angew. Chem. Int. Ed. 38 (1999) 1088.
[24] O. Castillo, A. Luque, P. Román, F. Lloret, M. Julve, Inorg. Chem. 40 (2001) 5526.
[25] Y.-Y. Zhang, M.-H. Zeng, Y. Qi, S.-Y. Sang, Z.-M. Liu, Inorg. Chem. Commun. 10 (2007) 33.
[26] S.J. Rettig, R.C. Thompson, J. Trotter, S.-H. Xia, Inorg. Chem. 38 (1999) 1360.
[27] S. Han, J.L. Manson, J. Kim, J.S. Miller, Inorg. Chem. 39 (2000) 4182.
[28] H.-H. Song, L.-M. Zheng, G.-S. Zhu, Z. Shi, S.-H. Feng, S. Gao, Z. Hu, X.-Q. Xin, J. Solid State Chem. 164 (2002) 367.
[29] S. Mandal, S.K. Pati, M.A. Green, S. Natarajan, Chem. Mater. 17 (2005) 638.
[30] D. Armentano, G. De Munno, F. Lloret, A.V. Palii, M. Julve, Inorg. Chem. 41 (2002) 2007.
[31] D. Armentano, G. De Munno, T.F. Mastropietro, M. Julve, F. Lloret, Chem. Commun. (2004) 1160.
[32] C.N.R. Rao, S. Natarajan, R. Vaidhyanathan, Angew. Chem. Int. Ed. 43 (2004) 1466.
[33] I. Dzyaloshinsky, J. Phys. Chem. Solids 4 (1958) 241.
[34] T. Moriya, Phys. Rev. 120 (1960) 91.
[35] R.L. Carlin, Magnetochemistry, Springer-Verlag, Berlin/Heidelberg, 1986, p. 149.